

- [6] H. Yang, N. Coombs, I. Sokolov, G. A. Ozin, *J. Mater. Chem.* **1997**, *7*, 1285.
- [7] I. A. Aksay, M. Trau, S. Manne, I. Honma, N. Yao, L. Zhou, P. Fenter, P. M. Eisenberger, S. M. Gruner, *Science* **1996**, *273*, 892.
- [8] M. Trau, N. Yao, E. Kim, Y. Xia, G. M. Whitesides, I. A. Aksay, *Nature* **1997**, *390*, 674.
- [9] R. Ryoo, C. Hyun Ko, S. J. Cho, J. M. Kim, *J. Phys. Chem. B* **1997**, *101*, 10610.
- [10] S. H. Tolbert, T. E. Schaffer, J. Feng, P. K. Hansma, G. D. Stucky, *Chem. Mater.* **1997**, *9*, 1962.
- [11] C. T. Kresge, M. E. Leonowicz, W. J. Roth, J. C. Vartuli, J. S. Beck, *Nature* **1992**, *359*, 710.
- [12] A. Monnier, F. Schüth, Q. Huo, D. Kumar, D. Margolese, R. S. Maxwell, G. D. Stucky, M. Krishnamurty, P. Petroff, A. Firouzi, M. Janicke, B. F. Chmelka, *Science* **1993**, *261*, 1299.
- [13] A. Firouzi, D. Kumar, L. M. Bull, T. Besier, P. Sieger, Q. Huo, S. A. Walker, J. A. Zasadzinski, C. Glinka, J. Nicol, D. Margolese, G. D. Stucky, B. F. Chmelka, *Science* **1995**, *267*, 1138.
- [14] J. S. Beck, J. C. Vartuli, W. J. Roth, M. E. Leonowicz, C. T. Kresge, K. D. Schmitt, C. T.-W. Chu, D. H. Olson, E. W. Sheppard, S. B. McCullen, J. B. Higgins, J. L. Schlenker, *J. Am. Chem. Soc.* **1992**, *114*, 10834.
- [15] S. A. Bagshaw, E. Prouzet, T. J. Pinnavaia, *Science* **1995**, *269*, 1242.
- [16] Q. Huo, D. I. Margolese, U. Ciesla, D. G. Demuth, P. Feng, T. E. Gier, P. Sieger, A. Firouzi, B. F. Chmelka, F. Schüth, G. D. Stucky, *Chem. Mater.* **1994**, *6*, 1176.
- [17] Q. Huo, D. I. Margolese, U. Ciesla, P. Feng, T. E. Gier, P. Sieger, R. Leon, P. M. Petroff, F. Schüth, G. D. Stucky, *Nature* **1994**, *368*, 317.
- [18] Q. Huo, D. I. Margolese, G. D. Stucky, *Chem. Mater.* **1996**, *8*, 1147.
- [19] I. Honma, H. S. Zhou, *Chem. Mater.* **1998**, *10*, 103.
- [20] I. Honma, H. Sasabe, H. S. Zhou, *Mater. Res. Soc. Symp. Proc.* **1997**, *457*, 525.
- [21] I. Honma, H. S. Zhou, *Adv. Mater.* **1998**, *10*, 1533.
- [22] H. S. Zhou, I. Honma, *Adv. Mater.* **1999**, *11*, 683.
- [23] H. S. Zhou, I. Honma, *J. Mater. Chem.* **1998**, *8*, 515.
- [24] D. Kundu, H. S. Zhou, I. Honma, *J. Mater. Sci. Lett.* **1998**, *17*, 2089.
- [25] X. S. Zhao, F. Audsley, G. Q. Lu, *J. Phys. Chem. B* **1998**, *102*, 4143.
- [26] H. Yang, N. Coombs, G. A. Ozin, *J. Mater. Chem.* **1998**, *8*, 1205.
- [27] K. Borisch, S. Diele, P. Goring, H. Kresse, C. Tschierske, *J. Mater. Chem.* **1998**, *8*, 529.
- [28] J. M. Seddon, R. H. Templer, *Philos. Trans. R. Soc. London A* **1993**, *377*.
- [29] K. Fontell, *Colloid Polym. Sci.* **1990**, *268*, 264.
- [30] P. J. Bruinsma, N. J. Hess, J. R. Bontha, J. Liu, S. Baskaran, *Mater. Res. Soc. Symp. Proc.* **1997**, *443*, 105.

Photorefractivity in Ferroelectric Liquid Crystal Composites Containing Electron Donor and Acceptor Molecules**

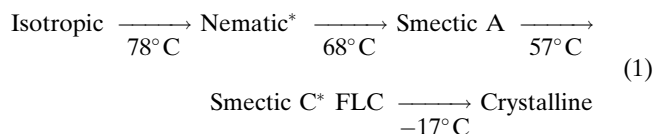
By Gary P. Wiederrecht, Beth A. Yoon, and Michael R. Wasielewski*

Traditional photorefractive materials, such as LiNbO₃ or BaTiO₃, are inorganic ferroelectric crystals.^[1,2] More recently, organic materials, including polymers,^[3-7] glasses,^[8] crystals,^[9] liquid crystals,^[10-16] and polymer/liquid crystal dispersions^[17-20] have been shown to exhibit the photore-

fractive effect: an orientational and/or electronic electro-optic response to a photoinduced space-charge field derived from a spatially periodic charge distribution within the material. Noticeably absent in the photorefractivity literature are ferroelectric liquid crystals (FLCs).^[21] Appropriately aligned FLCs have a net polarization (P_S) in the smectic C* phase and also have C₂ symmetry that permits, in principle, the observation of electronic electro-optic effects that are not possible in nematic liquid crystals.^[22,23] Additionally, FLCs can illustrate orientational effects that are not derived solely from quadratic coupling of the space-charge field to the dielectric anisotropy ($\Delta\epsilon$), but to coupling of P_S to the space-charge field—a potentially far stronger orientational effect than is possible in nematic liquid crystals.

We present here the first observation of photorefractivity in FLCs. These results are possible because of dopant chromophores chosen for the optimal free energy for charge separation to produce mobile ions,^[24] and careful control of the wavevector and light polarization relative to the smectic liquid crystal planes. The electron donor is perylene (PER), which absorbs visible light and donates an electron from its lowest excited singlet state to N,N'-(di-n-butyl)pyromellitimide (PI), an easily reduced molecule that has no visible absorption bands. The concentration of PER = 2×10^{-3} M and PI = 4×10^{-3} M. This produces an anisotropic absorption coefficient of $\alpha \sim 1 \text{ cm}^{-1}$ measured using s-polarized light (vide infra).

The FLC used is a eutectic mixture, CS-1015, commercially available from Chisso Corporation, Japan, which has a phase transition diagram as follows:



CS-1015 has a polarization of -6.6 nC/cm^2 and an index of refraction anisotropy of $\Delta n = 0.14$. In order to obtain aligned FLC films, we used commercially available cells (Displaytech) with a 4 μm spacing that have a rubbed polyimide layer designed to align FLCs. The doped liquid crystal was placed at the edge of the cell in the isotropic phase at 90 °C and drawn into the cell through capillary action. The cell was then slowly cooled at 0.5 °C/h to room temperature.

The FLC aligns in a manner that depends largely on the spacer thickness and the pitch length of the FLC. The different alignment possibilities are a result of the well-known helical pattern of FLCs, in which the polarization of the molecules rotates in a helical pattern with a pitch length typically on the order of a few micrometers.^[22,25] An homogeneously aligned FLC will possess a precessing director (\mathbf{n}) perpendicular to the planes of the Sm C* liquid crystal. This produces a rotating spontaneous polarization (P_S) and no macroscopic polarization. However, at a relatively low applied field ($\sim 1 \text{ V}/\mu\text{m}$), the helix can be unwound and the molecular dipoles can align with the field.^[26] This produces the “bookshelf” geometry, where the long axes of the molecules are aligned parallel to

[*] Prof. M. R. Wasielewski, Dr. B. A. Yoon
Department of Chemistry, Northwestern University
Evanston, IL 60208-3113 (USA)
E-mail: wasielew@chem.nwu.edu

Dr. G. P. Wiederrecht
Chemistry Division, Argonne National Laboratory
Argonne, IL 60439-4831 (USA)

[**] The authors gratefully acknowledge support from the Office of Advanced Scientific Computing Research, Technology Research Division, DOE under contract W-31-109-ENG-38 (GPW) and the Office of Naval Research under Grant No. N00014-99-1-0411 (MRW).

the plane of the glass slides, with a tilt angle θ from the rubbing axis. The molecular dipole is oriented perpendicular to the long axis of the FLC molecules and points toward the face of the cell, which produces macroscopic polarization in the material.^[27]

To study the photorefractive effect in this doped FLC we use Ar⁺ laser output at 514 nm that is split into two beams of 15 mW each. The beams are overlapped at an angle $\theta' = 8^\circ$ at the sample to create an optical interference pattern with a grating spacing of $\Lambda = 2.1 \mu\text{m}$, Figure 1. An applied voltage of up to 22 V is used, producing an applied field E_A up to $5.5 \text{ V}/\mu\text{m}$. The sample is tilted relative to the bisector of the beams by $\beta = 32.5^\circ$. This induces directional charge transport along the wavevector of the optical interference pattern, so that spatial modulation of the charge distribution is possible. The inset illustrates the optical interference and the relative orientation of the FLC molecules in an applied field, for the applied field normal to the plane of the page. The angle ϕ is the rotation angle of the cell about an axis normal to the surface of the cell walls. The writing beams are s-polarized, i.e., perpendicular to the wavevector, and no photorefractive beam coupling was observed for p-polarized beams. This contrasts with the observation that only p-polarized beams lead to beam coupling in homeotropically aligned liquid crystals, consistent with different director orientation in FLCs.^[10,11] Finally, no beam coupling was observed in the absence of an applied field or without tilting the cell relative to the bisector of the writing beams. The photoconductivity (σ_{\parallel}) of the cell with 22 V applied is $4.5 \times 10^{-12} \Omega^{-1} \text{ cm}^{-1}$, while the dark conductivity is $9 \times 10^{-13} \Omega^{-1} \text{ cm}^{-1}$.

The values for $\Lambda = 2.1$ and $4 \mu\text{m}$ cell thickness produce a quality value (Q), a measure of the degree of Bragg character of the grating, of ~ 2 . Since Q values of ~ 10 are required to produce true Bragg gratings, this grating possesses a degree of Raman-Nath (thin grating) character. In the thin grating regime, the use of a photorefractive gain coefficient ($I \propto e^{-\Gamma d}$, where I is intensity, Γ is the gain coefficient, and d is the optical path length) has been debated, with some groups reporting an exponential gain coefficient.^[10,12,28] We choose here to report only a beam coupling ratio, i.e., I_{12}/I_1 where I_{12} is the intensity of beam one in the presence of beam 2 and I_1 is the intensity of beam one in the absence of beam two.

The conductivity and nonlinear optical effects should be highly anisotropic, so that the relative orien-

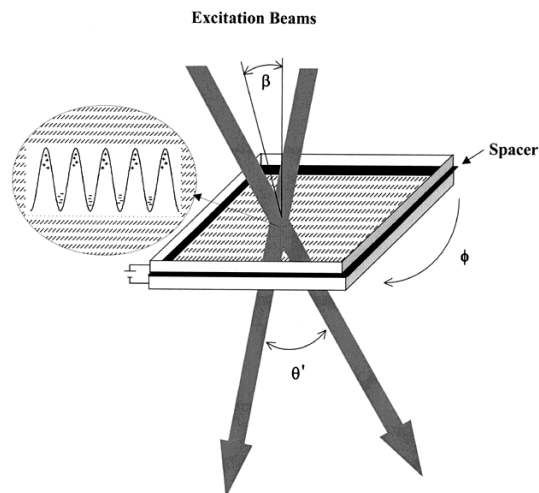


Fig. 1. A schematic of the experimental geometry is illustrated. The sample is tilted at an angle $\beta = 32.5^\circ$ relative to the bisector of the two beams. This allows charge migration along the grating wavevector, which results in a sinusoidal space-charge field. The beams are polarized perpendicular to the grating wavevector. The planes of the smectic C* FLC can be rotated by an angle ϕ relative to the wavevector direction.

tation of the smectic planes relative to the wavevector of the optical interference pattern should produce changes in the photorefractive beam coupling ratio. Figure 2 illustrates the beam coupling ratio as a function of the rotation angle ϕ of the cell. Also illustrated is the transmission of one of the

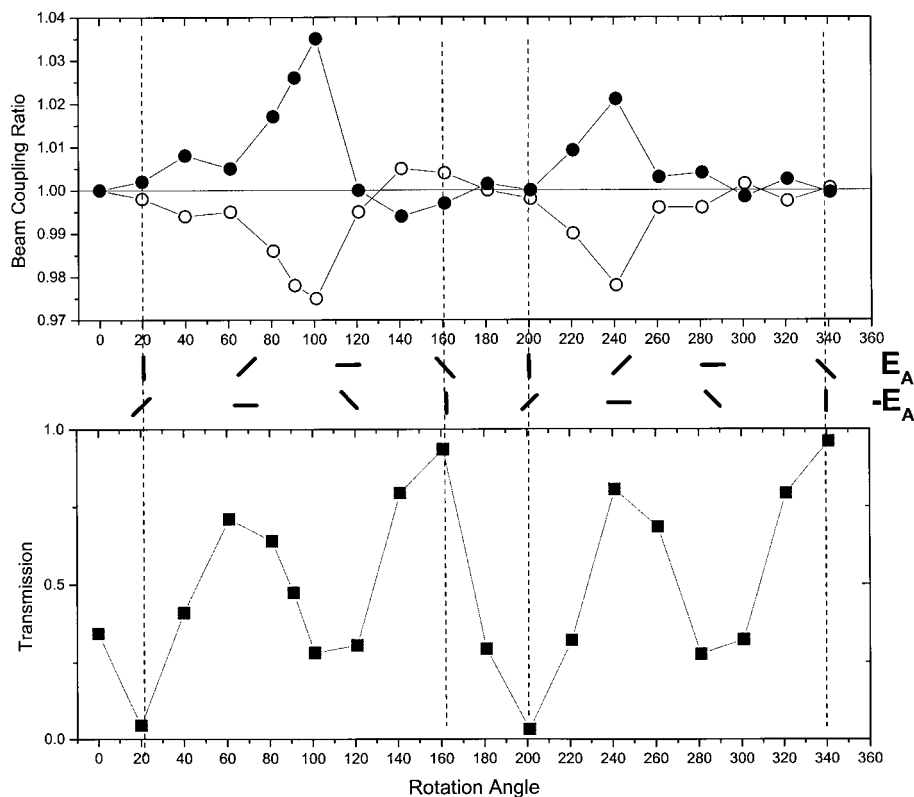


Fig. 2. The dependence of beam coupling ratio on the rotation angle ϕ is shown. Also shown is the transmission through cross polarizers of a vertically polarized beam for an applied field E_A at which beam coupling ratio is observed compared to the transmission at $-E_A$. The relative orientations of the molecules are shown for E_A and $-E_A$.

beams through cross polarizers, so that the relative orientation of the molecules relative to the wavevector can be determined. At 0° and 180°, the smectic planes and the wavevector of the optical interference pattern are parallel. The orientation of the molecules is illustrated between the two graphs for the applied field E_A at which the beam coupling is measured and the second row of orientations is for the opposite polarity $-E_A$. Since the polarization of the writing beams is perpendicular to the wavevector, the maximum extinction, i.e., when the molecular orientation is parallel to the polarization of the writing beams, is at $\phi = 20^\circ$ or 200° .

Figure 2 shows a spike in the beam coupling ratio at $\phi = 100^\circ$ and a smaller spike at $\phi = 240^\circ$. For most of the rotation angles ϕ , no significant beam coupling is observed. In the region around 100° where maximum beam coupling is observed, the FLC molecules are oriented with their long axis nearly perpendicular to the polarization of the writing beams and parallel to the wavevector of the grating. This provides some clues as to the electro-optic and space-charge field buildup mechanisms. First, for $\phi = 100^\circ$, charge migration along the wavevector is approximately parallel to the FLC director. The magnitude of E_{SC} for diffusing ions has the following space-charge field dependence:^[11]

$$E_{SC} = \left(\frac{-k_B TK}{2e_0} \right) \left(\frac{D^+ - D^-}{D^+ + D^-} \right) \left(\frac{\sigma_{ph}}{\sigma_{ph} + \sigma_d} \right) \times \sin Kx \quad (2)$$

Here, σ_{ph} is the photoconductivity, σ_d is the dark conductivity, k_B is the Boltzmann constant, K is the grating wavevector, x is the direction along the wavevector, e_0 is the charge of the electron, and D^+ and D^- are the diffusion constants for the cations and anions, respectively. This equation assumes that the intensities of the two incident beams are equal ($I_1 = I_2$). It is clear that the two factors that determine the magnitude of the space-charge field are the difference in the photoconductivity versus dark conductivity and the difference in the diffusion coefficients of the cations and anions. Previous experimental results provide precedent for the high mobility of one charge carrier in FLCs, supporting the ability of FLCs to possess a spatially periodic charge distribution.^[29] The diffusion of the more mobile species is maximized at this orientation, with ions moving approximately parallel to the long molecular axis.

Our results indicate that the photorefractive electro-optic mechanism is derived from orientational effects and not the linear electro-optic effect. First, the majority of FLCs have a small degree of electronic second-order nonlinear character, as measured by small electro-optic coefficients (r_{ij}) that are 1–2 orders of magnitude lower than their crystalline counterparts.^[30] The few exceptions are FLCs that utilize molecules with large hyperpolarizabilities aligned along the polar axis.^[23,30,31] Second, the r_{22} coefficient dominates the electronic electro-optic mechanism in FLCs.^[23,30] In this tilted geometry, accessing r_{22} would require the writing beams to be p-polarized where no photorefractivity is observed. The s-polarized beams are consistent with an orientational response, because the maximum signal is obtained when the molecules are aligned nearly perpendicular to the light polar-

ization. In this region, an angular change of the molecular orientation produces the largest change in the index of refraction as a component of the long axis begins to align with the light polarization.

Although orientational photorefractivity is still dominant in FLCs as with nematic liquid crystals, the mechanism for orientational coupling to the space-charge field is different. As stated above, the reorientation of the molecules in FLCs can occur through a coupling to the polarization, i.e., proportional to PE_{SC} , as opposed to nematic liquid crystals in which the reorientation is coupled solely to the dielectric anisotropy ($\Delta\epsilon$), proportional to $\Delta\epsilon E_{SC}^2$. Figure 3 shows the dependence of the beam coupling ratio on applied voltage, which is far less than

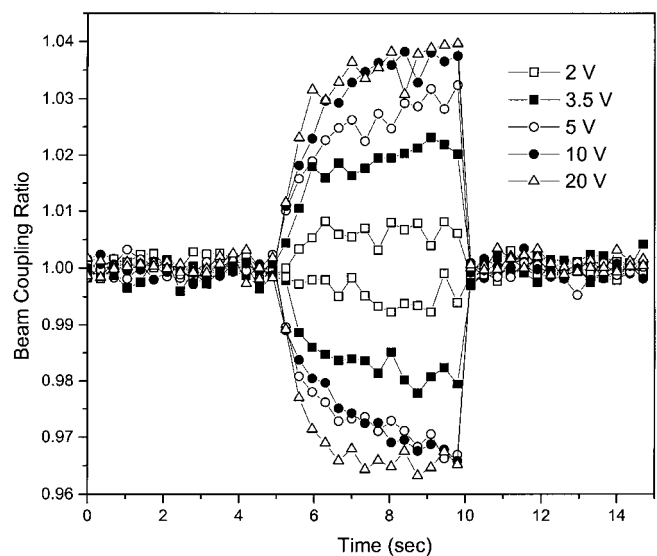


Fig. 3. The dependence of the beam coupling ratio on applied voltage is illustrated.

the $(V_A E_{SC})^2$ dependence of diffraction efficiency previously shown for nematic liquid crystals (V_A is the applied voltage).^[10] The beam coupling ratio in the FLC composite is saturated for an applied voltage of 10 V, but larger applied voltages give faster grating formation times.

The reorientational capabilities of the FLC director in response to a switch in the polarity of the applied field could lead to novel possibilities for on/off switching of the photorefractive effect. Since we have shown that the photorefractive effect in FLCs is strongly correlated with the alignment of the FLC molecules relative to the writing beam polarization, a reorientation of the molecules in response to a polarity switch in the applied field could act to quickly increase or decrease the beam coupling ratio in FLC composites. Figure 4 shows the beam coupling changes for an orientation of 100° , where photorefractivity is maximized for an applied voltage of 22 V. At 10 s, the voltage is switched to -22 V for 5 s. The signal is corrected for a small change in the transmission, when the polarity switch occurs. A rapid decrease in the beam coupling is observed, consistent with a molecular reorientation of 45° to a region where less photorefractivity is observed. This is followed by a slower erasure of the modulated space-charge field

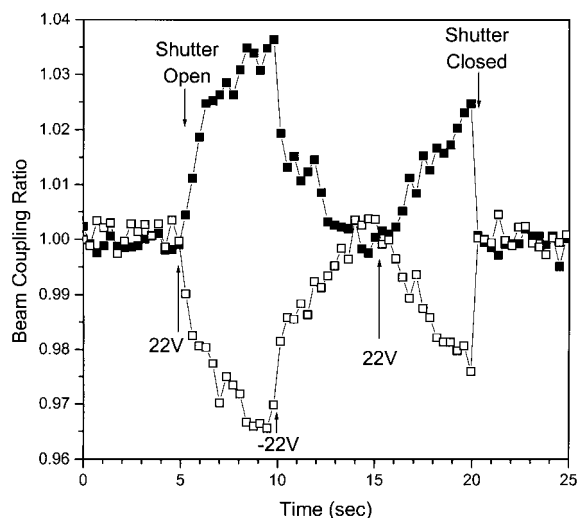


Fig. 4. The change of the beam coupling ratio when the applied voltage is switched from 22 V to -22 V is shown. The rapid initial decrease is due to the reorientation of the FLC director to a less optimal orientation for photorefractivity. The slower change is due to the erasure of the space-charge field.

as charges begin to redistribute in response to the applied field polarity change. At 20 s, the voltage is switched back to 22 V, and the initial charge modulation begins to reform.

We have observed for the first time orientational photorefractivity in FLC composites containing easily oxidized and reduced chromophores. The applied field dependence suggests that the orientational response is a result of the space-charge field coupling to the bulk polarization of the FLC and not to dielectric anisotropy as with nematic liquid crystals. In order to increase the likelihood of observing the linear electronic electro-optic effect in addition to orientational contributions, one possibility is to use homeotropically aligned FLCs with a transverse applied field, so that the modulated space-charge field lies along the polar axis of the FLC. The use of FLCs specifically designed to increase P_S and the electronic electro-optic effect would also prove advantageous for improving the performance of these novel materials.

Received: April 27, 2000

[1] A. Ashkin, G. D. Boyd, J. M. Dziedzic, R. G. Smith, A. A. Ballman, J. J. Lexinstein, K. Nassau, *Appl. Phys. Lett.* **1966**, *9*, 72.
 [2] P. Gunter, J. P. Huignard, *Photorefractive Materials and Their Applications I: Fundamental Phenomena*, Springer, Berlin **1988**.
 [3] S. Ducharme, J. C. Scott, R. J. Twieg, W. E. Moerner, *Phys. Rev. Lett.* **1991**, *66*, 1846.
 [4] W. E. Moerner, A. Grunnet-Jepsen, C. L. Thompson, *Annu. Rev. Mater. Sci.* **1997**, *27*, 585.
 [5] K. Meerholz, B. L. Volodin, Sandalphon, B. Kippelen, N. Peyghambarian, *Nature* **1994**, *371*, 497.
 [6] L. Yu, W. K. Chan, A. Peng, A. Gharavi, *Acc. Chem. Res.* **1996**, *29*, 13.
 [7] J. G. Winiarz, L. Zhang, M. Lal, C. S. Friend, P. N. Prasad, *J. Am. Chem. Soc.* **1999**, *121*, 5287.
 [8] P. M. Lundquist, R. Wortmann, C. Geletnky, R. J. Twieg, M. Jurich, V. Y. Lee, C. R. Moylan, D. M. Burland, *Science* **1996**, *274*, 1182.
 [9] K. Sutter, J. Hulliger, R. Schlessler, P. Gunter, *Opt. Lett.* **1993**, *18*, 778.
 [10] I. C. Khoo, H. Li, Y. Liang, *Opt. Lett.* **1994**, *19*, 1723.
 [11] E. V. Rudenko, A. V. Sukhov, *JETP Lett.* **1994**, *59*, 142.
 [12] G. P. Wiederrecht, B. A. Yoon, M. R. Wasielewski, *Science* **1995**, *270*, 1794.
 [13] H. Ono, I. Saito, N. Kawatsuki, *Appl. Phys. Lett.* **1998**, *72*, 1942.
 [14] S. Bartkiewicz, A. Miniewicz, F. Kajzar, M. Zagorska, *Appl. Opt.* **1998**, *37*, 6871.

[15] G. Cipparrone, A. Mazzulla, F. Simoni, *Opt. Lett.* **1998**, *23*, 1505.
 [16] N. V. Tabiryan, C. Umeton, *J. Opt. Soc. Am. B* **1998**, *15*, 1912.
 [17] A. Golemme, B. L. Volodin, B. Kippelen, N. Peyghambarian, *Opt. Lett.* **1997**, *22*, 1226.
 [18] H. Ono, *Opt. Lett.* **1997**, *22*, 1144.
 [19] G. P. Wiederrecht, M. R. Wasielewski, *J. Am. Chem. Soc.* **1998**, *120*, 3231.
 [20] J. Zhang, K. D. Singer, *Appl. Phys. Lett.* **1998**, *72*, 2948.
 [21] R. B. Meyer, L. Liebert, L. Strzelecki, P. Keller, *J. Phys. Lett.* **1975**, *36*, 69.
 [22] N. A. Clark, S. T. Lagerwall, *Appl. Phys. Lett.* **1980**, *36*, 899.
 [23] J.-Y. Liu, M. G. Robinson, K. M. Johnson, D. M. Walba, M. B. Ros, N. A. Clark, R. Shao, D. Doroski, *J. Appl. Phys.* **1991**, *70*, 3426.
 [24] G. P. Wiederrecht, B. A. Yoon, M. R. Wasielewski, *Adv. Mater.* **1996**, *8*, 535.
 [25] I. Cuculescu, A. L. Alexe-Ionescu, R. Bena, C. Ghizdeanu, V. Stoian, G. Barbero, A. T. Ionescu, *Mod. Phys. Lett. B* **1995**, *9*, 791.
 [26] B. I. Ostrovski, A. Z. Rabinovich, V. G. Chigrinov, in *Advances in Liquid Crystal Research and Applications* (Ed: L. Bata), Pergamon, Oxford **1980**.
 [27] C. Escher, R. Wingen, *Adv. Mater.* **1992**, *4*, 189.
 [28] D. D. Nolte, D. H. Olson, G. E. Doran, W. W. Knox, A. M. Glass, *J. Opt. Soc. Am. B* **1990**, *7*, 2217.
 [29] B. Maximus, E. D. Ley, A. D. Meyere, H. Pauwels, *Ferroelectrics* **1991**, *121*, 103.
 [30] M. Trollsas, C. Orrenius, F. Sahlen, U. W. Gedde, T. Norin, A. Hult, D. Hermann, P. Rudquist, L. Komitov, S. T. Lagerwall, J. Lindstrom, *J. Am. Chem. Soc.* **1996**, *118*, 8542.
 [31] H. Kapitza, R. Zentel, R. J. Twieg, C. Nguyen, S. U. Vallerien, F. Kremer, C. G. Willson, *Adv. Mater.* **1990**, *11*, 539.

Flexible Smart Window via Surface Graft Copolymerization of Viologen on Polyethylene

By Jeyagowry Thirugnana Sampanthar, Koon Gee Neoh,* Sock Wee Ng, En Tang Kang, and Kuang Lee Tan

The development of chromogenic materials for glazing “smart” or “intelligent” windows has been actively pursued in recent years. The change in the optical properties of these materials may be activated by electricity, heat, or light. Examples of commonly used chromogenic materials are certain transition-metal oxides such as WO_3 , NiO, MoO_3 , and organic compounds such as viologens, diphthalocyanines, and polyaniline.^[1–5] The viologens are among the most studied chromogenic materials and the change in coloration is achieved by an oxidation–reduction reaction. However, since the short-chain viologens are soluble in water, various methods of synthesizing viologen-containing chromogenic systems have been developed. These include the incorporation of viologens into anionic polyelectrolyte films,^[6] iminodiacetic acid-type chelate resin beads,^[7] and *N*-vinyl-2-pyrrolidone-methyl acrylate copolymers,^[8] as well as the casting of ruthenium(II) complex and viologen containing partially quarternized poly(1-vinylimidazole) into films.^[9]

* Prof. K. G. Neoh, Dr. J. T. Sampanthar, S. W. Ng, Prof. E. T. Kang
 Department of Chemical & Environmental Engineering
 National University of Singapore
 Kent Ridge 119260 (Singapore)
 E-mail: chenkg@nus.edu.sg
 Prof. K. L. Tan
 Department of Physics
 National University of Singapore
 Kent Ridge 119260 (Singapore)